Survival probability of random walks and Lévy flights on a semi-infinite line

Satya Majumdar, Philippe Mounaix, Gregory Schehr

Survival Probability of Random Walks and Lévy Flights on a Semi-Infinite Line

Satya N. Majumdar,[1,*] Philippe Mounaix,[2,†] and Grégory Schehr[1,‡]

[1] *LPTMS, CNRS, Univ. Paris-Sud, Université Paris-Saclay, 91405 Orsay, France*
[2] *Centre de Physique Théorique, Ecole Polytechnique, CNRS, Université Paris-Saclay, F-91128 Palaiseau, France*

We consider a one-dimensional random walk (RW) with a continuous and symmetric jump distribution, $f(\eta)$, characterized by a Lévy index $\mu \in (0, 2]$, which includes standard random walks ($\mu = 2$) and Lévy flights ($0 < \mu < 2$). We study the survival probability, $q(x_0, n)$, representing the probability that the RW stays non-negative up to step n, starting initially at $x_0 \geq 0$. Our main focus is on the x_0-dependence of $q(x_0, n)$ for large n. We show that $q(x_0, n)$ displays two distinct regimes as x_0 varies: (i) for $x_0 = O(1)$ ('quantum' regime), the discreteness of the jump process significantly alters the standard scaling behavior of $q(x_0, n)$ and (ii) for $x_0 = O(n^{1/\mu})$ ('classical' regime) the discrete-time nature of the process is irrelevant and one recovers the standard scaling behavior (for $\mu = 2$ this corresponds to the standard Brownian scaling limit). The purpose of this paper is to study how precisely the crossover in $q(x_0, n)$ occurs between the quantum and the classical regime as one increases x_0.

* majumdar@lptms.u-psud.fr
† philippe.mounaix@cpht.polytechnique.fr
‡ gregory.schehr@lptms.u-psud.fr

I. INTRODUCTION

Consider a simple Brownian walker on a line whose position $x(t)$ evolves, starting initially at $x_0 > 0$, in continuous time via the Langevin equation

$$\frac{dx}{dt} = \eta(t) \tag{1}$$

where $\eta(t)$ is a Gaussian white noise with zero mean and a correlator $\langle \eta(t)\eta(t')\rangle = 2\,D\,\delta(t-t')$. Let $q(x_0,t)$ denote the probability that the walker does not cross zero up to time t, starting at $x_0 > 0$ at $t = 0$. This is called the persistence or the survival probability of the walker and has been extensively studied in the literature [1–5]. In fact, $q(x_0,t)$ satisfies a backward Fokker-Planck equation where one considers x_0 as a variable [3, 4]

$$\frac{\partial q(x_0,t)}{\partial t} = D\,\frac{\partial^2 q(x_0,t)}{\partial x_0^2} \tag{2}$$

valid for $x_0 \geq 0$ with the absorbing boundary condition $q(x_0 = 0, t) = 0$ at the origin and with the initial condition $q(x_0 > 0, t = 0) = 1$. The solution is simply

$$q(x_0,t) = \mathrm{erf}\left(\frac{x_0}{\sqrt{4\,D\,t}}\right); \quad \text{where} \quad \mathrm{erf}(z) = \frac{2}{\sqrt{\pi}}\int_0^z e^{-u^2}\,du\,. \tag{3}$$

Using $\mathrm{erf}(z) \approx 2z/\sqrt{\pi}$ as $z \to 0$, it follows that for any fixed $x_0 \geq 0$, the survival probability at late times decays as a power law

$$q(x_0,t) \sim \frac{x_0}{\sqrt{\pi D t}} \qquad \text{for } t \to +\infty. \tag{4}$$

Thus, for any fixed $x_0 \geq 0$, the walker eventually crosses the origin when the time t exceeds the characteristic diffusion time $t^* = x_0^2/2D$. In particular, if the walker starts at the origin $x_0 = 0$, $t^* = 0$ and the walker dies immediately with probability 1. In other words, $q(x_0 = 0, t) = 0$ at all times. This shows up in any typical Brownian trajectory starting at the origin at $t = 0$. It immediately crosses and re-crosses the origin infinitely often, making it impossible for the walker to survive (see Fig. 1 a) for a typical Brownian trajectory).

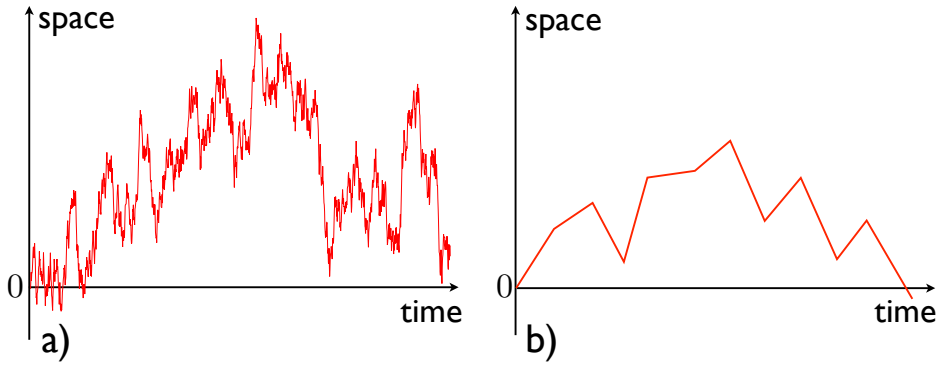

FIG. 1. **a):** Typical trajectory of a Brownian motion (1) starting from the origin $x_0 = 0$. It immediately crosses and re-crosses the origin infinitely often, yielding a vanishing survival probability $q(x_0,t)$, as in Eq. (4). **b)** Typical trajectory of a discrete-time random walk starting from the origin $x_0 = 0$ and staying positive right after. Since the walker can travel for several steps before first crossing the origin, the survival probability $q(0,n)$ is finite, as in Eq. (9).

Consider now a random walker on a line that evolves in discrete time by making random independent jumps at each time step. Starting from the initial position x_0, the position of the walker now evolves in discrete time via the simple Markov jump rule

$$x_n = x_{n-1} + \eta_n \tag{5}$$

where η_n represents the random jump at step n. The jump lengths η_n's are assumed to be independent and identically distributed (i.i.d.) random variables, each drawn from a continuous and symmetric probability distribution function

(PDF), $f(\eta)$, the Fourier transform of which

$$\hat{f}(k) = \int_{-\infty}^{\infty} f(\eta)\, e^{ik\eta}\, d\eta \tag{6}$$

is assumed to have the following small-k behavior

$$\hat{f}(k) = 1 - (a_\mu\, |k|)^\mu + \dots \tag{7}$$

where $0 < \mu \leq 2$ and a_μ represents a typical length scale associated with the jump. The Lévy exponent $0 < \mu \leq 2$ dictates the large $|\eta|$ tail of $f(\eta)$. For jump PDF's with a finite second moment $\sigma^2 = \int_{-\infty}^{\infty} \eta^2\, f(\eta)\, d\eta$, such as Gaussian, exponential, uniform etc, one evidently has $\mu = 2$ and $a_2 = \sigma/\sqrt{2}$. In contrast, $0 < \mu < 2$ corresponds to jump densities with fat tails $f(\eta) \sim |\eta|^{-1-\mu}$ as $|\eta| \to \infty$, generally called Lévy flights with index μ (for reviews on these jump processes see [6, 7]).

Let $q(x_0, n)$ now denote the persistence, or survival probability, of this discrete-time walker starting at $x_0 \geq 0$ up to time n. Unlike in the continuous-time Brownian motion and as a consequence of the discrete-time dynamics of the jump process, there is now a finite fraction of trajectories starting at $x_0 = 0$ that travel several steps before first crossing the origin to the negative side [see Fig. 1 b)], yielding a non-zero $q(x_0 = 0, n)$ at any finite n. For a continuous and symmetric $f(\eta)$, $q(0, n)$ is given by the universal Sparre Andersen formula [8]

$$q(0, n) = \binom{2n}{n} 2^{-2n} \tag{8}$$

which decays algebraically for large times n as

$$q(0, n) \sim \frac{1}{\sqrt{\pi\, n}} \qquad \text{for } n \to +\infty. \tag{9}$$

Let us emphasize that the results in Eqs. (8) and (9) are completely universal, i.e, independent of $f(\eta)$ and the $1/\sqrt{n}$ algebraic decay holds for all Lévy flights with index $0 < \mu \leq 2$.

The comparison between Eqs. (4) and (9) raises some questions. Consider, for instance, a discrete-time walk with jumps of finite variance σ^2, i.e. with index $\mu = 2$ and $a_2 = \sigma/\sqrt{2}$ in Eq. (7). For such a walk, central limit theorem tells us that the discrete-time process $x(n)$ converges for large n to the continuous-time Brownian motion $x(t)$, upon identifying $2\, D\, t = \sigma^2 n$. Hence, the persistence $q(x_0, n)$ should converge to the Brownian motion result. As a result, one may naively replace t by $n\sigma^2/2D$ in the Brownian result in Eq. (4) and conclude that the $1/\sqrt{n}$ decay given by the Sparre Andersen theorem in Eq. (9) is basically the same as the $1/\sqrt{t}$ decay of persistence for the Brownian motion. There are however two problems with this simplistic picture: (i) the $1/\sqrt{n}$ behavior in Eq. (9) holds not just for Brownian motion, but also for Lévy flights with divergent σ^2 (i.e., $\mu < 2$) which do not converge to Brownian motion at late times. Hence the $1/\sqrt{n}$ decay in Sparre Andersen theorem has a different origin than the $1/\sqrt{t}$ decay of the Brownian persistence. (ii) More importantly, the Brownian persistence vanishes when $x_0 \to 0$ in Eq. (4), i.e., $q(x_0 = 0, t) = 0$, while the persistence $q(x_0, n)$ for the discrete-time jump process remains finite even when $x_0 = 0$ (as in Eq. (9)). So, how would it be possible to reconcile between these seemingly different results for persistence in the discrete and continuous time processes?

The resolution to this puzzle is actually simple. There are two ways to take the continuous time limit of the discrete-time persistence $q(x_0, n)$ for jump PDF's with finite variance σ^2. Either one fixes x_0 and takes the limits $n \to \infty$ and $\sigma^2 \to 0$ keeping the product $\sigma^2\, n = 2\, D\, t$ fixed, where t is the continuous time, or one fixes σ^2 and scales $x_0 \sim \sqrt{n}$ for large n in order to converge to the Brownian result. Essentially, what matters is that the ratio $x_0/\sqrt{\sigma^2\, n}$ should be kept $O(1)$. Let us work with fixed σ^2. Then, the Brownian result in Eq. (3) is recovered only in the scaling limit when $x_0 \sim \sqrt{n}$, i.e., for large x_0. For $x_0 = O(1)$, there is no convergence to the Brownian limit, hence the universal result $q(x_0, n) \sim 1/\sqrt{\pi\, n}$ as $x_0 \to 0$ (Sparre Andersen limit) has nothing to do with the $1/\sqrt{t}$ Brownian decay which holds only when $x_0 \sim \sqrt{n}$.

One is then faced with the following question: how precisely does the large n behavior of $q(x_0, n)$ as a function of x_0 (for jump processes with a finite σ^2) cross over from the Sparre Andersen limit ($x_0 \to 0$) to the Brownian limit ($x_0 \sim \sqrt{n}$) as x_0 is increased? The main purpose of this paper is to address this question. We will show that there are indeed two different scales of x_0, namely $x_0 = O(1)$ and $x_0 \sim n^{1/2}$, where the large n scaling behaviors of $q(x_0, n)$ are very different. We will call the first regime (with $x_0 = O(1)$) the *discrete 'quantum'* regime, as the discrete-time nature of the process plays a dominant role in this regime. In contrast the second regime (with $x_0 \sim n^{1/2}$) will be referred to as the *'classical'* scaling regime, i.e., the usual Brownian scaling regime. A similar picture of two separated scales of x_0 appears for jump processes with a divergent σ^2 (i.e., Lévy flights with $0 < \mu < 2$). Here again the large n

behavior of $q(x_0,n)$ is different in the two regimes: $x_0 = O(1)$ (discrete 'quantum' regime), and $x_0 \sim n^{1/\mu}$ ('classical' scaling regime). This latter regime reduces to the Brownian scaling regime if $\mu = 2$. In this paper, we will study $q(x_0,n)$ for general $0 < \mu \leq 2$. We will compute the large n behavior of $q(x_0,n)$ in both 'quantum' and standard scaling regimes and we will demonstrate how the rather different results in these two regimes match smoothly as x_0 is increased from $O(1)$ to $O(n^{1/\mu})$.

This clarification of the asymptotic behavior of $q(x_0,n)$ in two widely separated scales of x_0 is particularly important in the light of several current applications of random walks, where the persistence probability $q(x_0,n)$ turns out to be a crucial ingredient or a building block. In fact, the earliest application of this half-space problem in presence of an absorbing boundary goes back to the celebrated 'Milne' problem in astrophysics in connection with the scattering of light from the sun's surface [9], and later a similar problem appeared in the theory of transport of neutrons through a non-capturing medium [10, 11]. In chemistry, the survival probability $q(x_0,n)$ is an important observable in the study of diffusion in presence of an absorbing boundary [12]. Amongst more recent applications, the knowledge of the asymptotic behavior of $q(x_0,n)$ was found to be crucial in computing the precise statistics of the global maximum of a random walk evolving via Eq. (5) [13] . Indeed, if one denotes by $x_{\max}$ the global maximum of a random walk evolving via Eq. (5) starting from the origin, the survival probability $q(x_0,n)$ actually coincides with the cumulative distribution of the maximum $x_{\max}$, i.e., Prob.$(x_{\max} \leq x_0) = q(x_0,n)$ [13, 14]. The same quantity $q(x_0,n)$ was also shown to appear in the problem of the capture of particles into a spherical trap in 3-dimension, known as the Smoluchowski problem [15, 16]. It also plays an important role in computing the order and gap statistics of a random walk sequence, e.g., in calculating the distribution of the gap between the k-th and the $(k+1)$-th maxima of a random walk sequence in Eq. (5) (see Refs. [18, 19]). Similarly, the joint distribution of the gap and time-lag between the highest and the second highest maximum, both for a discrete-time random walk sequence in Eq. (5), as well as for the so called continuous-time random walk (CTRW), requires a precise knowledge of $q(x_0,n)$ [20–23]. Finally, $q(x_0,n)$ is at the heart of fluctuation theory [1, 24] and plays a major role in the statistics of records and associated observables in several correlated time-sequences generated from the basic simple random walk sequence in Eq. (5) [1, 24–30] (for a recent review on record statistics, see Ref. [31]). Hence clarifying the precise asymptotic properties of $q(x_0,n)$ in different regimes of x_0 is important and crucial.

Let us remark that many results on the asymptotic properties of $q(x_0,n)$ for large n are already known, in particular in the limit $x_0 = 0$ (see e.g. Ref. [1, 2, 4, 8]) and in the scaling regime when $x_0 \sim n^{1/\mu}$ for large n (see for instance, Refs. [13–15, 26]). However, how these two asymptotic behaviors match precisely as x_0 increases from $O(1)$ to $O(n^{1/\mu})$ has not been clearly elucidated yet, to the best of our knowledge, for general jump processes with $0 < \mu \leq 2$. This issue was briefly addressed in Ref. [15] in a somewhat different context (see also Ref. [14] for a discussion), but only for the special case of exponential jump distribution, i.e., $f(\eta) = (1/2)\, e^{-|\eta|}$. This paper gathers in one place the scattered literature on $q(x_0,n)$ for a Lévy flight, with arbitrary $0 < \mu \leq 2$, on a semi-infinite line in the presence of an absorbing boundary at the origin and present a unifying picture that demonstrates the matching of $q(x_0,n)$ across the two widely separated scales of x_0, i.e. $x_0 = O(1)$ and $x_0 = O(n^{1/\mu})$. While the spirit of this manuscript is thus more of a review, there are nevertheless some new results as well, a list of which can be found in the concluding section.

The rest of the paper is organized as follows. In Section II, we summarize our main results. In Section III, we provide the general setting for calculating the survival probability using the Pollaczek-Spitzer formula. In Section IV, we discuss the discrete quantum regime when $x_0 = O(1)$. In Section V, we consider the classical scaling regime. Finally, we conclude with a discussion and a list of the new results in Section VI. Some technical details of the computations are relegated to the Appendices A and B.

II. SUMMARY OF MAIN RESULTS

In this Section we summarize our main results. We consider the large n behavior of the persistence $q(x_0,n)$ for arbitrary, *symmetric and continuous* jump PDF $f(\eta)$ whose Fourier transform $\hat{f}(k)$ behaves for small-k as in Eq. (7), with Lévy index $0 < \mu \leq 2$. We find two different scaling behaviors depending on whether $x_0 = O(1)$ (discrete quantum regime) or $x_0 \sim n^{1/\mu}$ (classical scaling regime). Namely, to leading order one has (see Fig. 2),

$$q(x_0,n) \sim \begin{cases} \dfrac{1}{\sqrt{n}}\, U(x_0) \quad \text{for} \quad n \to +\infty \quad \text{and} \quad x_0 = O(1)\ , \\ \\ V_\mu\left(\dfrac{x_0}{n^{1/\mu}}\right) \quad \text{for} \quad n \to +\infty \quad \text{and} \quad x_0 = O(n^{1/\mu})\ . \end{cases} \tag{10}$$

The function $U(x_0)$ is given by its Laplace transform

$$\int_0^\infty U(x_0)\, e^{-\lambda\, x_0}\, dx_0 = \frac{1}{\lambda\,\sqrt{\pi}}\, \exp\left[-\frac{\lambda}{\pi}\int_0^\infty \frac{dk}{\lambda^2+k^2}\, \ln\left(1-\hat{f}(k)\right)\right]\ , \tag{11}$$

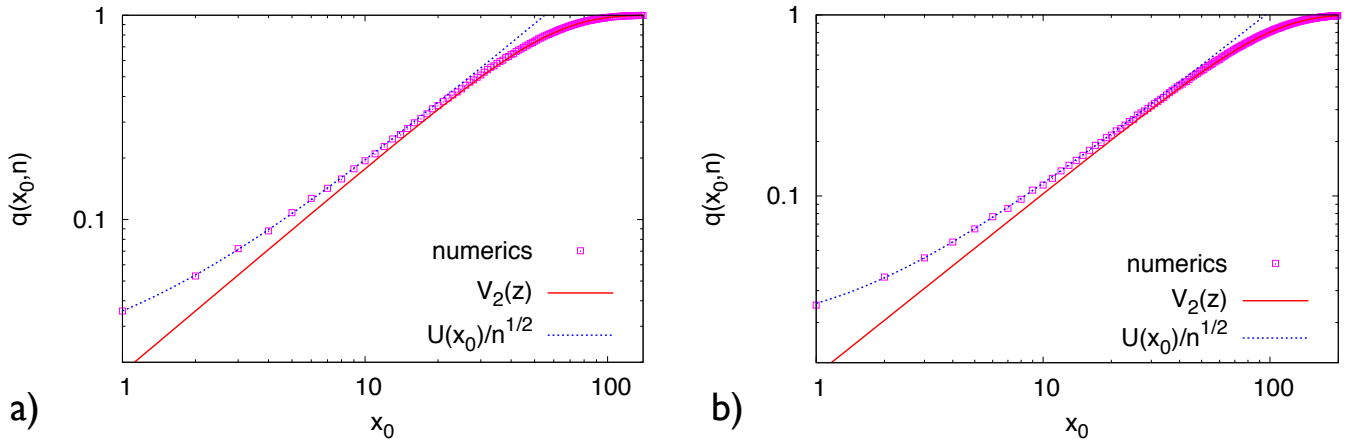

FIG. 2. **a)** Log-log plot of $q(x_0, n)$ for the exponential jump distribution $f(\eta) = (1/2)e^{-|\eta|}$ and $n = 1000$ steps. The squares represent numerical results. The solid red line corresponds to $V_2(z = x_0/\sqrt{n})$ given in Eq. (21) with $a_2 = 1$ while the dotted blue line corresponds to $U(x_0)/\sqrt{n}$ with $U(x_0)$ given in Eq. (72) with $a = 1$. **b)** The same quantity as in the left panel, $q(x_0, n)$, plotted on a log-log plot for a gamma jump distribution $f(\eta) = (1/2)|\eta|\, e^{-|\eta|}$ and $n = 1000$ steps. The solid red line corresponds to $V_2(z = x_0/\sqrt{n})$ given in Eq. (21) with $a_2 = \sqrt{3}$ while the dotted blue line corresponds to $U(x_0)/\sqrt{n}$ with $U(x_0)$ given in Eq. (77) with $a = \sqrt{3}$. These plots clearly illustrate the two different regimes for $x_0 = O(1)$ and $x_0 = O(\sqrt{n})$ as well as the crossover from the former to the latter as x_0 increases past $x_0 \sim 30$.

where $\hat{f}(k)$ is the Fourier transform of the jump PDF $f(\eta)$. Thus, $U(x_0)$ depends on the full $\hat{f}(k)$ and not just on its small-k expansion (7). For notational convenience, we will not make this dependence explicit and simply write $U(x_0)$ (instead of, e.g., $U_{[\hat{f}]}(x_0)$). The scaling function $V_\mu(z)$, by contrast, depends only on the small k behavior of $\hat{f}(k)$ in Eq. (7) and hence can be labelled just by the index μ. (Note that $U(x_0)$ cannot be labelled just by μ as it depends on the full $\hat{f}(k)$ and not just its small-k behavior). We show that $V_\mu(z)$ is given by the following double integral transform

$$\int_0^\infty dy\, e^{-y}\, y^{1/\mu} \int_0^\infty dz\, V_\mu(z)\, e^{-w\, y^{1/\mu}\, z} = \frac{1}{w}\, J_\mu(w)\ , \quad \text{where } J_\mu(w) = \exp\left[-\frac{1}{\pi}\int_0^\infty \frac{du}{1+u^2}\, \ln\left(1 + (a_\mu\, w\, u)^\mu\right)\right]\ . \tag{12}$$

While it is not easy to invert these integral transforms for a generic jump PDF $f(\eta)$ (except in some special cases, see later), it is possible to derive the large and small argument asymptotic behaviors of $U(x_0)$ and $V_\mu(z)$ explicitly. For $U(x_0)$, we find

$$U(x_0) \sim \begin{cases} \alpha_0 + \alpha_1\, x_0 + O(x_0^2) & \text{as } x_0 \to 0 \\ \\ A_\mu\, x_0^{\mu/2} + T_\mu(x_0) & \text{as } x_0 \to \infty\ , \end{cases} \tag{13}$$

where $T_\mu(x_0) = o(x_0^{\mu/2})$ as $x_0 \to \infty$. The constants in Eq. (13) are explicitly given by

$$\alpha_0 = \frac{1}{\sqrt{\pi}}\ , \tag{14}$$

$$\alpha_1 = -\frac{1}{\pi^{3/2}}\int_0^\infty dk\, \ln\left(1 - \hat{f}(k)\right)\ , \tag{15}$$

$$A_\mu = \frac{a_\mu^{-\mu/2}}{\sqrt{\pi}\,\Gamma(1+\mu/2)}\ . \tag{16}$$

The large x_0 behavior of $T_\mu(x_0)$ is rather difficult to analyze explicitly for an arbitrary value of μ, as it depends on the small-k behavior of $\hat{f}(k)$ beyond the leading order (7), involving higher order corrections $\hat{f}(k) = 1 - (a_\mu|k|)^\mu + c\,(a_\mu|k|)^\alpha + \ldots$, with $\alpha > \mu$. However, in the case where $\hat{f}(k)$ is an analytic function at $k = 0$, i.e. $\hat{f}(k) = 1 - (a_2 k)^2 + O(k^4)$ (corresponding thus to $\mu = 2$ and $\alpha = 4$), one can show that $T_2(x_0) \to B_2$ as $x_0 \to \infty$, where B_2 is a computable constant. In this case, the second line of Eq. (13) reduces to

$$U(x_0) \sim A_2\, x_0 + B_2 + O(1/x_0) \quad \text{as} \quad x_0 \to \infty \tag{17}$$

with $A_2 = 1/a_2\sqrt{\pi}$ and

$$B_2 = -\frac{1}{a_2\,\pi^{3/2}} \int_0^\infty \frac{dk}{k^2}\, \ln\left[\frac{1-\hat{f}(k)}{(a_2\,k)^2}\right], \tag{18}$$

which can be rewritten as

$$U(x_0) \sim \frac{1}{a_2\,\sqrt{\pi}}\,[x_0 + C_2] \quad \text{as} \quad x_0 \to \infty \tag{19}$$

with

$$C_2 = a_2\sqrt{\pi}\,B_2 = -\frac{1}{\pi} \int_0^\infty \frac{dk}{k^2}\, \ln\left[\frac{1-\hat{f}(k)}{(a_2\,k)^2}\right]. \tag{20}$$

Interestingly, this same constant C_2 has also appeared in a number of other contexts before, such as in the correction term to the expected maximum of a random walk [13, 32], in the Smoluchowski trapping problem for Rayleigh flights in three dimensions [15–17] and as the so called "Hopf constant" in the physics of radiative transfer [9–11, 33]. For a discussion of this constant in another interesting context, see subsection IV A.

We now consider the scaling function $V_\mu(z)$ for $0 < \mu \leq 2$. It turns out that for $\mu = 2$, one can derive the scaling function $V_2(z)$ exactly for all z. One finds

$$V_2(z) = \mathrm{erf}\left(\frac{z}{2\,a_2}\right), \tag{21}$$

which is consistent with the Brownian result in Eq. (3) once $2\,D\,t$ is replaced with $\sigma^2\,n = a_2^2\,n/2$, as expected for $\mu = 2$. From Eq. (21) one gets the asymptotic behaviors

$$V_2(z) \sim \begin{cases} \dfrac{1}{a_2\sqrt{\pi}}\,z & \text{as } z \to 0 \\ \\ 1 - \dfrac{2\,a_2}{\sqrt{\pi}z}\,e^{-z^2/4\,a_2^2} & \text{as } z \to \infty\,. \end{cases} \tag{22}$$

For $0 < \mu < 2$, the analysis of the scaling function $V_\mu(z)$ is a little bit more complicated. Here, we provide the dominant asymptotic behaviors only,

$$V_\mu(z) \sim \begin{cases} A_\mu\,z^{\mu/2} & \text{as } z \to 0 \\ \\ 1 - \tilde{A}_\mu\,z^{-\mu} & \text{as } z \to \infty\,, \end{cases} \tag{23}$$

where A_μ is the same as in Eq. (16) and

$$\tilde{A}_\mu = \frac{a_\mu^\mu}{\pi}\,\Gamma(\mu)\,\sin\left(\frac{\mu\pi}{2}\right) \qquad \text{with } 0 < \mu < 2\,. \tag{24}$$

Using the aforementioned connection between $q(x_0, n)$ and the cumulative distribution of the global maximum $x_{\max}$, it is possible to relate $V_\mu(z)$ with the PDF of the maximum of a stable process, $v_\mu(z)$, which has been well studied in the mathematical literature (see e.g. [34] and references therein). Indeed, in the scaling regime n and $x \to +\infty$ with fixed $x/n^{1/\mu}$ one has Prob.$(x_{\max} = x) \sim n^{-1/\mu} v_\mu(x/n^{1/\mu})$, which yields $V_\mu(z) = \int_0^z v_\mu(z')\,dz'$. Note in particular that for $\mu = 1$, the PDF $v_1(z)$ can be computed exactly [35], providing thus an explicit integral representation of the scaling function $V_1(z)$ in this special case

$$V_1(z) = \frac{1}{\pi} \int_0^z dz'\, \frac{1}{z'^{1/2}(1+z')^{3/4}}\, \exp\left(-\frac{1}{\pi}\int_0^{z'} dw\, \frac{\ln w}{1+w^2}\right). \tag{25}$$

It can be checked that the asymptotics given above in Eq. (23) are fully compatible with the known series expansion of $v_\mu(z)$ [34].

Finally, it can be seen that the leading order behaviors of $q(x_0, n)$ in the two regimes considered in Eq. (10) match smoothly near their common limit of validity. Indeed, taking the large x_0 limit in the inner regime ($x_0 = O(1)$) where

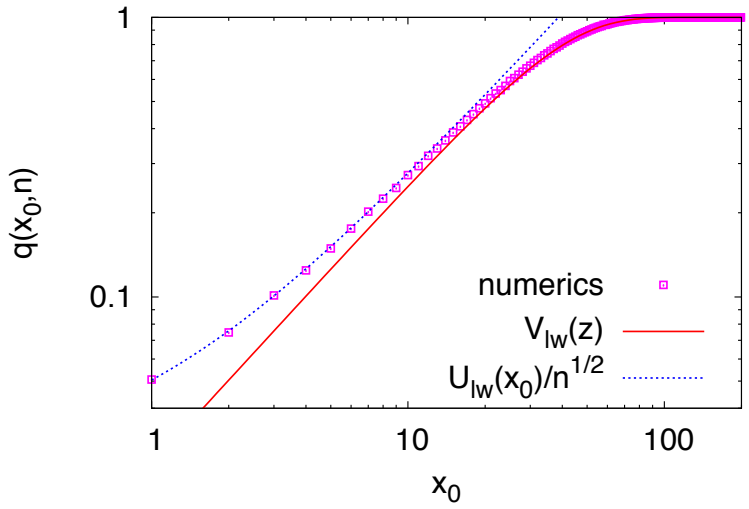

FIG. 3. Log-log plot of $q(x_0, n)$ for the the lattice random walk (with lattice constant 1), i.e. $f(\eta) = \frac{1}{2}\delta(\eta-1) + \frac{1}{2}\delta(\eta+1)$ and $n = 1000$ steps. The squares represent numerical results. The solid red line corresponds to $V_{\rm lw}(z = x_0/\sqrt{n})$ given in Eq. (28) while the dotted blue line corresponds to $U_{\rm lw}(x_0)/\sqrt{n}$ with $U_{\rm lw}(x_0)$ given in Eq. (27). As for continuous jump distributions (see Fig. 2), this plot for the lattice random walk clearly illustrates the two different regimes for $x_0 = O(1)$ and $x_0 = O(\sqrt{n})$ as well as the crossover from the former to the latter as x_0 increases past $x_0 \sim 30$.

$q(x_0, n) \approx U(x_0)/\sqrt{n}$ in Eq. (10) and using the large x_0 behavior of $U(x_0)$ in Eq. (13), one gets $q(x_0, n) \simeq A_\mu\, x_0^\mu/\sqrt{n}$. Similarly, taking the small $x_0/n^{1/\mu}$ limit in the outer regime ($x_0 = O(n^{1/\mu})$) where $q(x_0, n) \approx V_\mu(x_0/n^{1/\mu})$ in Eq. (10) and using the small z behavior of $V_\mu(z)$ in Eq. (23), one obtains exactly the same result, $q(x_0, n) \simeq A_\mu\, x_0^\mu/\sqrt{n}$, ensuring a smooth matching between the two scales.

Note that the main results mentioned above in Eqs. (10) to (12) hold for symmetric and *continuous* jump PDF $f(\eta)$ only. A natural example that does not belong to this class of continuous jump densities is the lattice random walk (with lattice constant 1) with ± 1 jumps, i.e, $f(\eta) = \frac{1}{2}\delta(\eta-1) + \frac{1}{2}\delta(\eta+1)$. While this jump PDF is symmetric, it is not continuous and hence our general formalism does not apply. However, we show in Appendix B that in this special case, the survival probability $q(x_0, n)$ (where x_0 is a non-negative integer) can be worked out explicitly. One finds in particular that the asymptotic behavior of $q(x_0, n)$ for large n also has a 'two scale' behavior (with $x_0 \sim O(1)$ and $x_0 \sim O(\sqrt{n})$) as a function of x_0, similar to the continuous jump PDF case in Eq. (10), albeit with different scaling functions. More precisely, we show in Appendix B that the counterpart of Eq. (10) in the ± 1 lattice random walk case is given by (see Fig. 3)

$$q(x_0, n) \sim \begin{cases} \dfrac{1}{\sqrt{n}}\, U_{\rm lw}(x_0) \quad \text{for} \quad n \to +\infty \quad \text{and} \quad x_0 = O(1)\ , \\ \\ V_{\rm lw}\left(\dfrac{x_0}{n^{1/2}}\right) \quad \text{for} \quad n \to +\infty \quad \text{and} \quad x_0 = O(n^{1/2})\ , \end{cases} \tag{26}$$

with

$$U_{\rm lw}(x_0) = \sqrt{\frac{2}{\pi}}\,(x_0+1) \quad \text{for all} \quad x_0 \geq 0\ , \tag{27}$$

$$V_{\rm lw}(z) = \text{erf}\left(\frac{z}{\sqrt{2}}\right)\ , \tag{28}$$

where the subscript 'lw' stands for lattice walk. One can again check that the behaviors of $q(x_0, n)$ match smoothly at the boundary between the two regimes in Eq. (26) (see Appendix-B for details).

III. SURVIVAL PROBABILITY FOR DISCRETE-TIME JUMP PROCESS: GENERAL SETTING

Consider the discrete-time jump process x_n defined in Eq. (5) for a symmetric and continuous jump PDF $f(\eta)$. The survival probability $q(x_0, n)$, starting at $x_0 \geq 0$, can be obtained from the 'constrained' propagator $p_+(y, n|x_0)$

which is the PDF for the random walker, starting at x_0, to be at y after n steps, staying above 0 in between. It is easy to see that $p_+(y,n|x_0)$ satisfies the following backward master equation

$$p_+(y,n|x_0) = \int_0^\infty p_+(y,n-1|x_1)\, f(x_1-x_0)\, dx_1 \ , \tag{29}$$

with the initial condition $p_+(y,0|x_0) = \delta(y-x_0)$. This Eq. (29) simply follows from the fact that in the first step, the walker jumps from $x_0 \geq 0$ to some $x_1 \geq 0$, staying positive, and then for the subsequent $(n-1)$ steps, the process renews with the new initial position at x_1. Finally, one has to integrate over all allowed positions $x_1 \geq 0$ where the walker can jump to in the first step. The initial condition follows immediately from the definition of $p_+(y,n|x_0)$. From the "constrained" propagator, the survival probability can be simply obtained as

$$q(x_0,n) = \int_0^\infty p_+(y,n|x_0)\, dy \ . \tag{30}$$

By integrating Eq. (29) over the final position y, one immediately obtains that the survival probability $q(x_0,n)$ also evolves via a backward master equation

$$q(x_0,n) = \int_0^\infty q(x_1,n-1)\, f(x_1-x_0)\, dx_1 \tag{31}$$

with the initial condition $q(x_0,n=0)=1$ for all $x_0 \geq 0$. Note that this master equation (31) can be directly obtained following the reasoning described below Eq. (29) and without using the constrained propagator $p_+(y,n|x_0)$.

The evolution equation (29) is deceptively simple but actually very hard to solve due to the integration extending over the semi-infinite interval $[0,\infty)$ only. It belongs to the general class of Wiener-Hopf integral equations which are notoriously not easy to solve for an arbitrary kernel $f(\eta)$. However, for the case where the kernel $f(\eta)$ has the interpretation of a probability density (i.e., non-negative for all arguments and normalizable to unity), there exists a solution to this equation which is given semi-explicitly by the so-called Hopf-Ivanov formula [36] (for a 'user friendly' derivation, see the Appendix A of Ref. [21])

$$\int_0^\infty dx_0 \int_0^\infty dy \sum_{n=0}^\infty p_+(y,n|x_0)\, s^n e^{-\lambda\, x_0 - \lambda'\, y} = \frac{\phi(s,\lambda)\, \phi(s,\lambda')}{\lambda+\lambda'} \ , \tag{32}$$

with

$$\phi(s,\lambda) = \exp\left[-\frac{\lambda}{\pi} \int_0^\infty \frac{\ln\left(1 - s\, \hat{f}(k)\right)}{\lambda^2 + k^2}\, dk \right] \ , \tag{33}$$

where $\hat{f}(k)$ is the Fourier transform of the jump PDF in Eq. (6). Setting $\lambda' = 0$ in Eq. (32) and using Eq. (30) one obtains a formula for the survival probability

$$\sum_{n=0}^\infty s^n \int_0^\infty q(x_0,n)\, e^{-\lambda\, x_0}\, dx_0 = \frac{\phi(s,\lambda)\phi(s,0)}{\lambda} \ . \tag{34}$$

The value $\phi(s,0)$ can be easily obtained from the expression in Eq. (33) by performing a change of variable $k = \lambda\, q$. Taking then the limit $\lambda \to 0$, using $\hat{f}(0) = 1$, one obtains that $\phi(s,0) = 1/\sqrt{1-s}$. Hence finally, one arrives at the so-called Pollaczek-Spitzer formula for the survival probability [37, 38]

$$\sum_{n=0}^\infty s^n \int_0^\infty q(x_0,n)\, e^{-\lambda\, x_0}\, dx_0 = \frac{1}{\lambda\sqrt{1-s}}\, \phi(s,\lambda) \ . \tag{35}$$

While the solution in Eq. (35) is exact, it is only semi-explicit in the sense that one needs to invert the Laplace transform as well as the generating function to obtain $q(x_0,n)$ fully explicitly. This is possible in some special cases only, e.g. for the exponential jump PDF $f(\eta) = e^{-|\eta|}/2$ [13, 15] (see Section IV B for other special cases). To derive the asymptotic properties of $q(x_0,n)$ from Eq. (35) is a nontrivial technical challenge which has been discussed in several articles [13–16, 18, 20, 26, 27, 30].

A remarkable simplification occurs if the starting point is exactly at the origin, i.e., $x_0 = 0$. By taking the limit $\lambda \to \infty$ in Eq. (35), it is easy to see that

$$\sum_{n=0}^\infty q(0,n)\, s^n = \frac{1}{\sqrt{1-s}} \ . \tag{36}$$

Thus, amazingly, the dependence on the jump PDF $f(\eta)$ disappears totally if $x_0 = 0$! This beautiful result goes by the name of the Sparre Andersen theorem [8]. Equating powers of s on both sides of Eq. (36), one gets

$$q(0,n) = \binom{2n}{n} 2^{-2n} \ , \tag{37}$$

a result that is completely *universal*, i.e., independent of $f(\eta)$, for all n. It follows in particular that, for large n,

$$q(0,n) \sim \frac{1}{\sqrt{\pi\, n}} \qquad \text{for } n \to +\infty, \tag{38}$$

which, obviously, is also universal. Let us emphasize again that this asymptotic result holds for any continuous and symmetric $f(\eta)$, including Lévy flights with $\mu < 2$.

In the next two sections we derive the large n behavior of $q(x_0, n)$ in the two different regimes $x_0 = O(1)$ and $x_0 = O(n^{1/\mu})$ respectively, using as a starting point the Pollaczek-Spitzer formula in Eq. (35).

IV. THE DISCRETE 'QUANTUM' REGIME $x_0 = O(1)$

Inverting Eq. (35) formally by using Cauchy's integral formula, one gets

$$\int_0^\infty q(x_0,n)\, e^{-\lambda\, x_0}\, dx_0 = \frac{1}{\lambda} \int_C \frac{ds}{2\pi i}\, \frac{1}{s^{n+1}}\, \frac{\phi(s,\lambda)}{\sqrt{1-s}}\,, \tag{39}$$

where the contour C goes counter-clockwise around $s = 0$ in the complex s-plane. From the expression of $\phi(s,\lambda)$ in Eq. (35), it can be checked that if $\lambda \neq 0$, then $\phi(s,\lambda)$ is an analytic function of s in the domain $|s| < 1 + \varepsilon$ for some $\varepsilon > 0$ and C can be deformed into a keyhole contour C' around the branch cut at $s = 1$. For large n, the integral is dominated by the contribution of C' near $s = 1$ and Eq. (39) reduces to

$$\int_0^\infty q(x_0,n)\, e^{-\lambda\, x_0}\, dx_0 \sim \frac{\phi(1,\lambda)}{\lambda} \int_{C'} \frac{ds}{2\pi i}\, \frac{1}{s^{n+1}}\, \frac{1}{\sqrt{1-s}} \qquad \text{for } n \to +\infty\,. \tag{40}$$

The s-integral in Eq. (40) is easily done by expanding $1/\sqrt{1-s}$ in a power series of s, applying the residue theorem for fixed n, and taking the limit $n \to +\infty$ in the result. One finds

$$\int_0^\infty q(x_0,n)\, e^{-\lambda\, x_0}\, dx_0 \sim \frac{1}{\sqrt{n}}\, \frac{\phi(1,\lambda)}{\lambda\,\sqrt{\pi}} \qquad \text{for } n \to +\infty, \tag{41}$$

and, by inverse Laplace transform,

$$q(x_0,n) \sim \frac{1}{\sqrt{n}}\, U(x_0) \qquad \text{for } n \to +\infty \text{ at fixed } x_0, \tag{42}$$

where $U(x_0)$ is defined by its Laplace transform

$$\int_0^\infty U(x_0)\, e^{-\lambda\, x_0}\, dx_0 = \frac{\phi(1,\lambda)}{\lambda\,\sqrt{\pi}} = \frac{1}{\lambda\,\sqrt{\pi}}\, \exp\left[-\frac{\lambda}{\pi} \int_0^\infty \frac{dk}{\lambda^2 + k^2}\, \ln\Big(1 - \hat{f}(k)\Big) \right]. \tag{43}$$

Here, we have used the expression of $\phi(s = 1, \lambda)$ from Eq. (35), which clearly shows that the function $U(x_0)$ depends on the full functional form of the jump PDF $f(\eta)$ through its Fourier transform $\hat{f}(k)$. It turns out that this function $U(x_0)$ satisfies a homogeneous integral equation,

$$U(x_0) = \int_0^\infty U(x_1)\, f(x_1 - x_0)\, dx_1, \tag{44}$$

which can be shown by substituting the form $q(x_0, n) = U(x_0)/\sqrt{n}$ directly into the backward equation (31). For a given $f(\eta)$, the homogeneous equation (44) has a unique solution up to an overall multiplicative constant which can be fixed from the Sparre Andersen limit, $U(x_0 = 0) = 1/\sqrt{\pi}$. Note however, that this solution is not that simple and is again given in terms of its Laplace transform only, as in Eq. (43).

A. Asymptotics of $U(x_0)$

Except in some particular cases (see e.g. the examples in Sec. IV B below), it is generally not possible to determine the full expression of $U(x_0)$ explicitly. Nevertheless, it is always possible to extract the small and large x_0 asymptotic behaviors of $U(x_0)$ from Eq. (43), as we will now show.

1. *The limit $x_0 \to 0$*

The small x_0 behavior of $U(x_0)$ is given by the large λ limit of the right-hand side (rhs) of Eq. (43). Expanding for large λ, one gets

$$\begin{aligned}\int_0^\infty U(x_0)\, e^{-\lambda\, x_0}\, dx_0 &= \frac{1}{\lambda\sqrt{\pi}}\, \exp\left[-\frac{1}{\pi\lambda}\, \int_0^\infty \ln\left(1-\hat{f}(k)\right)\, dk + O\left(\frac{1}{\lambda^2}\right)\right] \\ &= \frac{1}{\lambda\sqrt{\pi}} - \frac{1}{\pi^{3/2}\lambda^2}\, \int_0^\infty \ln\left(1-\hat{f}(k)\right)\, dk + O\left(\frac{1}{\lambda^3}\right), \end{aligned} \tag{45}$$

and by inverse Laplace transform, one finds the following small x_0 behavior

$$U(x_0) = \alpha_0 + \alpha_1\, x_0 + O(x_0^2) \tag{46}$$

where the constants α_0 and α_1 are given in Eqs. (14) and (15) respectively. Note that Eqs. (42) and (46) yield $q(x_0=0,n) \sim \alpha_0/\sqrt{n}$ $(n \to +\infty)$ with $\alpha_0 = 1/\sqrt{\pi}$ independent of $f(\eta)$, which coincides precisely with the universal Sparre Andersen limit in Eq. (38), as it should be.

2. *The limit $x_0 \to \infty$*

The large x_0 behavior of $U(x_0)$ is given by the small λ limit of the rhs of Eq. (43), which is a bit more subtle to analyze. Before letting λ go to zero, first we need to separate out the most singular term. To this end, we note that $\hat{f}(k) \sim 1 - (a_\mu\, |k|)^\mu$ as $k \to 0$, and we write

$$\ln\left[1-\hat{f}(k)\right] = \ln\left[\frac{1-\hat{f}(k)}{(a_\mu\, k)^\mu}\, (a_\mu\, k)^\mu\right] = \mu\, \ln(a_\mu\, k) + \ln\left[\frac{1-\hat{f}(k)}{(a_\mu\, k)^\mu}\right], \tag{47}$$

on the rhs of Eq. (43). Using then the identity

$$\int_0^\infty \frac{dk}{\lambda^2+k^2}\, \ln(a_\mu\, k) = \frac{\pi}{2\lambda}\, \ln(a_\mu\, \lambda)\,, \tag{48}$$

we get

$$\int_0^\infty U(x_0)\, e^{-\lambda\, x_0}\, dx_0 = \frac{1}{\sqrt{\pi}\, a_\mu^{\mu/2}\, \lambda^{1+\mu/2}}\, \exp\left[-K(\lambda)\right]\ ;\ \text{where } K(\lambda) = \frac{\lambda}{\pi}\int_0^\infty \frac{dk}{\lambda^2+k^2}\, \ln\left[\frac{1-\hat{f}(k)}{(a_\mu\, k)^\mu}\right]. \tag{49}$$

Note that, so far, we have not taken the $\lambda \to 0$ limit. We have just re-written the rhs of Eq. (43) in a way that will make it possible to control this $\lambda \to 0$ limit in Eq. (49). In particular, one can show that $K(\lambda) = O(\lambda^{\zeta(\mu)})$ as $\lambda \to 0$, with $0 < \zeta(\mu) \leq 1$. Thus, for small λ one has

$$\int_0^\infty U(x_0)\, e^{-\lambda\, x_0}\, dx_0 = \frac{1}{\sqrt{\pi}\, a_\mu^{\mu/2}\, \lambda^{1+\mu/2}}\, \left[1 + O(\lambda^{\zeta(\mu)})\right], \tag{50}$$

and by inverse Laplace transform, one obtains the large x_0 behavior

$$U(x_0) = A_\mu\, x_0^{\mu/2} + T_\mu(x_0)\,, \tag{51}$$

as announced in the second line of Eq. (13), with $T_\mu(x_0) = o(x_0^{\mu/2})$ for large x_0, and where the constant A_μ is given in Eq. (16). The analysis of the function $T_\mu(x_0)$ is more complicated as it depends on the small k behavior (7) of $\hat{f}(k)$,

but also on the exponent α associated with the first correction to this leading behavior $\hat{f}(k) \approx 1-(a_\mu|k|)^\mu+c\,(a_\mu|k|)^\alpha$. We omit these details here, though they are straightforward to compute.

Instead we focus on the case where $\hat{f}(k)$ is analytic at $k=0$, so that its small-k expansion reads

$$\hat{f}(k) = 1 - (a_2\,k)^2 + c\,(a_2 k)^4 + \cdots \,. \tag{52}$$

We start from Eq. (49) which is valid for general $\hat{f}(k)$. Setting $\mu = 2$ and using Eq. (52) it is to see that, to leading order as $\lambda \to 0$,

$$K(\lambda) \to \frac{\lambda}{\pi}\int_0^\infty \frac{dk}{k^2}\,\ln\left[\frac{1-\hat{f}(k)}{(a_2\,k)^2}\right] . \tag{53}$$

Note that this integral is convergent both in the infrared and the ultraviolet regimes. Therefore, keeping only the two leading terms in Eq. (49) gives

$$\int_0^\infty U(x_0)\,e^{-\lambda x_0}\,dx_0 \sim \frac{1}{\sqrt{\pi}\,a_2\,\lambda^2}\left(1-\frac{\lambda}{\pi}\int_0^\infty \frac{dk}{k^2}\,\ln\left[\frac{1-\hat{f}(k)}{(a_2\,k)^2}\right]\right) . \tag{54}$$

Inverting this Laplace transform term by term, we get

$$U(x_0) \sim A_2\,x_0 + B_2 + O(1/x_0) \quad \text{as} \quad x_0 \to \infty \tag{55}$$

with

$$A_2 = 1/a_2\sqrt{\pi}\,, \qquad B_2 = -\frac{1}{a_2\,\pi^{3/2}}\int_0^\infty \frac{dk}{k^2}\,\ln\left[\frac{1-\hat{f}(k)}{(a_2\,k)^2}\right] . \tag{56}$$

Let us rewrite Eq. (55), using the expressions of A_2 and B_2 from Eq. (56), as

$$U(x_0) \sim \frac{1}{a_2\,\sqrt{\pi}}\,[x_0 + C_2] \quad \text{as} \quad x_0 \to \infty \tag{57}$$

with

$$C_2 = a_2\sqrt{\pi}\,B_2 = -\frac{1}{\pi}\int_0^\infty \frac{dk}{k^2}\,\ln\left[\frac{1-\hat{f}(k)}{(a_2\,k)^2}\right] . \tag{58}$$

This constant C_2 has the following interpretation. For $\hat{f}(k)$ that is analytic at $k=0$, the asymptotic behaviors of $U(x_0)$ are given by

$$U(x_0) \sim \begin{cases} \frac{1}{\sqrt{\pi}} + O(x_0) & \text{as } x_0 \to 0 \\ \\ \frac{1}{a_2\,\sqrt{\pi}}\,[x_0 + C_2] & \text{as } x_0 \to \infty\,, \end{cases} \tag{59}$$

with C_2 given in Eq. (58). The function $U(x_0)$, when plotted versus x_0, is asymptotically linear for large x_0. If we extrapolate this asymptotic large x_0 linear behavior all the way to $x_0 < 0$, it has a negative intercept at $x_0 = -C_2$ (see Fig. 4). The survival probability $q(x_0, n) \sim U(x_0)/\sqrt{n}$, if extrapolated to negative x_0, vanishes at $x_0 = -C_2$. While the actual value $q(0,n) \sim 1/\sqrt{\pi\,n}$ is nonzero at the origin $x_0 = 0$, the far-away profile instead indicates an effective location of the absorbing origin at $x_0 = -C_2$. In the context of the physics of radiative transfer, this constant C_2 is known as the Milne extrapolation length [9, 10]. This constant has also appeared in the Smoluchowski trapping problem for Rayleigh flights in three dimensions [15] and also in the subleading asymptotic large n behavior of the expected maximum of a random walk of n steps [13, 15, 32].

In the context of radiative transfer of photons, the appropriate jump distribution turns out to be [9, 10, 33]

$$f(\eta) = \frac{1}{2}\int_0^1 \frac{du}{u}\,e^{-|\eta|/u}\,, \tag{60}$$

which is known as the Milne kernel. For this particular kernel, the constant C_2 came to be known as the Hopf constant $C_2^{\rm Hopf}$ [11]. Calculating $C_2^{\rm Hopf}$ has a long history, going back to Hopf who first computed it numerically,

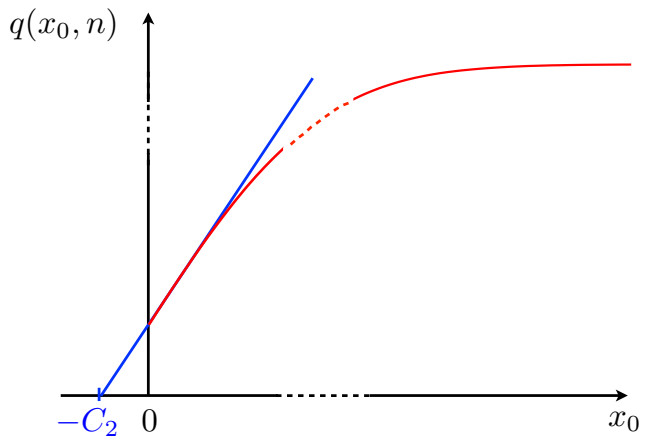

FIG. 4. Sketch of a plot of $q(x_0, n)$ (red line) as a function of x_0 (in arbitrary units along both axes). The blue line corresponds to $U(x_0)/\sqrt{n}$ as in Eq. (10). The large x_0 behavior of $U(x_0)/\sqrt{n}$ [see Eq. (59)], when extrapolated to negative x_0, vanishes at $x_0 = -C_2$.

finding $C_2^{\rm Hopf} \approx 0.710$. A decade later a team of physicists working in the Manhattan project needed a more accurate value to find the critical mass of Uranium [33], and $C_2^{\rm Hopf}$ was then computed to many decimal places. There indeed exists an analytical expression for this constant in terms of the so called Chandrasekhar H-function defined as [39, 40]

$$H(z) = \exp\left[-\frac{z}{\pi}\int_0^\infty \ln\left(1 - \frac{\tan^{-1}\lambda)}{\lambda}\right)\frac{d\lambda}{1+z^2\lambda^2}\right] . \tag{61}$$

The Hopf constant $C_2^{\rm Hopf}$ is then given by [11]

$$C_2^{\rm Hopf} = \frac{\sqrt{3}}{2}\int_0^1 H(z)\, z^2\, dz = 0.7104460895\ldots\ . \tag{62}$$

Using a different method, Placzek and Seidel give an alternative and more compact analytical expression for the Hopf constant [10],

$$C_2^{\rm Hopf} = \frac{6}{\pi^2} + \frac{1}{\pi}\int_0^{\pi/2}\left[\frac{3}{x^2} - \frac{1}{1 - x\cot x}\right] dx = 0.7104460895\ldots\ . \tag{63}$$

Yet another analytical expression for $C_2^{\rm Hopf}$ can be derived from our Eq. (58). Using the Milne jump distribution in (60), we find that its Fourier transform is given by

$$\hat{f}(k) = \frac{\tan^{-1} k}{k} , \tag{64}$$

which, for small-k, behaves as $\hat{f}(k) = 1 - k^2/3 + \cdots$, giving $a_2 = 1/\sqrt{3}$ [see Eq. (7)]. Plugging this in Eq. (58), we get the following expression for the Hopf constant

$$C_2^{\rm Hopf} = -\frac{1}{\pi}\int_0^\infty \frac{dk}{k^2}\ln\left[\frac{3}{k^2}\left(1 - \frac{\tan^{-1} k}{k}\right)\right] = 0.7104460895\ldots\ . \tag{65}$$

We remark that in the notation of this paper, the Chandrasekhar H-function can be expressed in terms of the function $\phi(s, \lambda)$ defined in Eq. (33). Using the expression of $\hat{f}(k)$ in Eq. (64), it is easy to check that

$$H(z) = \phi(1, 1/z) . \tag{66}$$

Here, we seemingly have three completely different analytical expressions for the Hopf constant $C_2^{\rm Hopf}$, respectively in Eqs. (62), (63) and (65). Proving that these analytical expressions are actually equivalent, which is not immediately evident, will be interesting in itself and as it might give an insight of possible links between the seemingly different methods used to derive these expressions.

B. Two exactly solvable cases

There are few special cases of jump PDF $f(\eta)$ for which the function $U(x_0)$ can be obtained explicitly by inverting Eq. (43). Here, we mention two examples in which such an inversion can be done.

Example I: Consider the symmetric exponential distribution

$$f(\eta) = \frac{1}{2a}\, e^{-|\eta|/a}\,, \tag{67}$$

where a is the typical jump length. Its Fourier transform is a Lorentzian

$$\hat{f}(k) = \frac{1}{1+a^2\,k^2}\,. \tag{68}$$

Substituting $\hat{f}(k)$ on the rhs of Eq. (43), one gets

$$\int_0^\infty U(x_0)\, e^{-\lambda\, x_0}\, dx_0 = \frac{1}{\lambda\sqrt{\pi}}\, \exp\left[-\frac{\lambda}{\pi}\int_0^\infty \frac{dk}{\lambda^2+k^2}\, \left(\ln(a^2\,k^2) - \ln(a^2\,k^2+1)\right)\right]\,. \tag{69}$$

The log-integrals appearing on the rhs of Eq. (69) can be performed explicitly using the following useful identity

$$\int_0^\infty \frac{dk}{\lambda^2+k^2}\, \ln(\alpha+\beta\,k^2) = \frac{\pi}{\lambda}\ln\left(\sqrt{\alpha}+\sqrt{\beta}\,\lambda\right)\,, \tag{70}$$

valid for any $\alpha \geq 0$ and $\beta \geq 0$. One obtains

$$\int_0^\infty U(x_0)\, e^{-\lambda\, x_0}\, dx_0 = \frac{1}{\sqrt{\pi}}\left(\frac{1}{\lambda}+\frac{1}{a\,\lambda^2}\right)\,, \tag{71}$$

which can now be trivially inverted to give

$$U(x_0) = \frac{1}{\sqrt{\pi}}\left(1+\frac{x_0}{a}\right)\,. \tag{72}$$

In Fig. 2 a), we show a plot of $U(x_0)/\sqrt{n}$ with $U(x_0)$ given in Eq. (72), and compare it to numerical simulations.

Example II: Consider now the symmetric gamma distribution of the form

$$f(\eta) = \frac{3\,|\eta|}{2\,a^2}\, e^{-\sqrt{3}\,|\eta|/a}\,. \tag{73}$$

The choice of the constants are such that the variance is $2a^2$. The Fourier transform of $f(\eta)$ can again be easily obtained

$$\hat{f}(k) = \left(1-\frac{k^2\,a^2}{3}\right)\,\left(1+\frac{k^2\,a^2}{3}\right)^{-2}\,, \tag{74}$$

which behaves, for small-k, as $\hat{f}(k) = 1 - a^2\,k^2$ as in Eq. (7) with $a_2 = a$. Substituting $\hat{f}(k)$ on the rhs of Eq. (43), and using again the identity in Eq. (70), one finds

$$\int_0^\infty U(x_0)\, e^{-\lambda\, x_0}\, dx_0 = \frac{1}{\sqrt{\pi}\, a\, \lambda^2\, (1+a\lambda/3)}\left(1+\frac{a\,\lambda}{\sqrt{3}}\right)^2\,. \tag{75}$$

Using now the following break-up into rational fractions

$$\frac{(1+b\lambda)^2}{\lambda^2(1+c\lambda)} = \frac{(b-c)^2}{1+c\lambda} + \frac{2b-c}{\lambda} + \frac{1}{\lambda^2}\,, \tag{76}$$

and Laplace inverting each term, one finally gets the explicit expression

$$U(x_0) = \frac{1}{\sqrt{\pi}}\,\left[\frac{2\sqrt{3}-1}{3} + \frac{x_0}{a} + \frac{(\sqrt{3}-1)^2}{3}\, e^{-3x_0/a}\right]\,. \tag{77}$$

In Fig. 2 b), we show a plot of $U(x_0)/\sqrt{n}$ with $U(x_0)$ given in Eq. (77), and compare it to numerical simulations.

Evidently, it can be checked that $U(x_0)$ in Eqs. (72) and (77) do satisfy the general asymptotic behaviors detailed in Eq. (13) (with $\mu = 2$ and $a_2 = a$). Additional numerical simulations, not shown here, confirm these asymptotic behaviors for other jump distributions, e.g. for a uniform and symmetric jump distribution, for which the full function $U(x_0)$ can not be computed explicitly.

V. THE 'CLASSICAL' SCALING REGIME $x_0 = O(n^{1/\mu})$

We now consider the survival probability in the scaling regime defined by $x_0 \sim n^{1/\mu}$ and large n. This scaling limit was already investigated in the context of the statistics of the number of records for multiple random walks and a derivation of Eq. (12) can be found in the appendices of Ref. [26]. There, the scaling function $V_\mu(z)$ was analyzed in the large z limit only. What we now need to understand the matching with the inner scale $x_0 = O(1)$ is the opposite limit $z \to 0$. In order to make this paper as self-contained as possible, we include a detailed derivation of Eq. (12) below and then provide the asymptotics of $V_\mu(z)$ both for $z \to 0$ and $z \to \infty$.

In the scaling limit, we need to take the limits $n \to \infty$ and $x_0 \to \infty$ keeping the ratio $z = x_0/n^{1/\mu}$ fixed in Eq. (35). In terms of the two conjugate variables s and λ, this scaling limit translates into taking the limits $s \to 1$ and $\lambda \to 0$ keeping the ratio $\lambda/(1-s)^{1/\mu}$ fixed. To proceed we set $p = 1-s$ in Eq. (35) and define the scaling variable $w = \lambda/p^{1/\mu}$. Let us first analyse the rhs of Eq. (35) in this scaling limit, in particular the function $\phi(s = 1-p, \lambda)$. Making the change of variable $k = \lambda u$ in the integral, we get

$$\phi(s = 1-p, \lambda) = \exp\left[-\frac{1}{\pi}\int_0^\infty \frac{du}{1+u^2}\,\ln\Big(1-(1-p)\,\hat{f}(\lambda u)\Big)\right]. \tag{78}$$

For $\lambda \to 0$ we can use the small-k expansion of $\hat{f}(k)$ in Eq. (7). Then, we write λ in terms of the scaled variable, $\lambda = w\,p^{1/\mu}$, where w is held fixed and $p \to 0$. This gives, to leading order in the scaling limit,

$$\phi(s = 1-p, \lambda = w\,p^{1/\mu}) \approx \exp\left[-\frac{1}{\pi}\int_0^\infty \frac{du}{1+u^2}\,\ln\left(p\,(1+(a_\mu\,w\,u)^\mu)\right)\right]. \tag{79}$$

Separating the $\ln p$ term and doing the integration, one gets

$$\phi(s = 1-p, \lambda = w\,p^{1/\mu}) \approx \frac{1}{\sqrt{p}}\,J_\mu(w); \quad \text{where } J_\mu(w) = \exp\left[-\frac{1}{\pi}\int_0^\infty \frac{du}{1+u^2}\,\ln\left(1+(a_\mu\,w\,u)^\mu\right)\right], \tag{80}$$

which, once substituted on the rhs of Eq. (35), yields the scaling limit

$$\sum_{n=0}^{\infty} e^{-p\,n}\int_0^\infty dx_0\,q(x_0,n)\,e^{-w\,p^{1/\mu}\,x_0} \sim \frac{1}{p^{1+1/\mu}}\,\frac{1}{w}\,J_\mu(w) \qquad \text{for } p \to 0 \text{ and fixed } w. \tag{81}$$

In order that both sides of Eq. (81) have the same scaling $\sim p^{-(1+1/\mu)}$ as $p \to 0$, it is clear that $q(x_0, n)$ must scale as

$$q(x_0, n) \sim V_\mu\left(\frac{x_0}{n^{1/\mu}}\right) \qquad \text{for} \quad n \to +\infty \quad \text{and} \quad x_0 \sim n^{1/\mu}\,. \tag{82}$$

To see this, we substitute the anticipated form (82) on the left-hand side (lhs) of Eq. (81), we write $y = p\,n$ and, in the limit $p \to 0$, we replace the sum over n by an integral over y. Rescaling then $x_0 = z n^{1/\mu} = z y^{1/\mu}\,p^{-1/\mu}$ we find that the lhs of Eq. (81) scales like $p^{-(1+1/\mu)}$ for $p \to 0$, as expected. Cancelling the factor $p^{-(1+1/\mu)}$ from both sides, gives the scaling function $V_\mu(z)$ as

$$\int_0^\infty dy\,e^{-y}\,y^{1/\mu}\int_0^\infty dz\,V_\mu(z)\,e^{-w\,y^{1/\mu}\,z} = \frac{1}{w}\,J_\mu(w); \quad \text{where } J_\mu(w) = \exp\left[-\frac{1}{\pi}\int_0^\infty \frac{du}{1+u^2}\,\ln\left(1+(a_\mu\,w\,u)^\mu\right)\right], \tag{83}$$

which is the main result of this section. Thus, the scaling function $V_\mu(z)$ depends on the jump PDF $f(\eta)$ only through the Lévy index $0 < \mu \leq 2$. We will now see that for $\mu = 2$, the expression of $V_2(z)$ can be obtained explicitly for all z, while for $0 < \mu < 2$, only the large and small z asymptotics of $V_\mu(z)$ can be obtained.

A. The case $\mu = 2$

For $\mu = 2$, the integral over u in the expression (83) of $J_2(w)$ can be performed exactly by using the identity in Eq. (70). One finds

$$\int_0^\infty dy\,e^{-y}\,y^{1/2}\int_0^\infty dz\,V_2(z)\,e^{-w\,y^{1/2}\,z} = \frac{1}{w\,(1+a_2\,w)}\,. \tag{84}$$

It is still not easy to invert Eq. (84). However, we know that for $\mu = 2$ and in this scaling regime, we must recover the Brownian result for $q(x_0, n)$ as given in Eq. (3) provided one replaces $2\,D\,t$ with $\sigma^2\,n = a_2^2 n/2$. This suggests that

$$V_2(z) = \mathrm{erf}\left(\frac{z}{2\,a_2}\right) . \tag{85}$$

It can now be checked by substituting Eq. (85) on the lhs of Eq. (84) and performing the integrals, that the explicit expression of $V_2(z)$ in Eq. (85) does indeed satisfy Eq. (84), which justifies this expression a posteriori.

B. The case $0 < \mu \leq 2$

For general $0 < \mu \leq 2$, it is hard to obtain $V_\mu(z)$ explicitly for all z from Eq. (83), except for $\mu = 1$ [see Eq. (25)]. In fact, for general μ, even extracting the asymptotic behavior of $V_\mu(z)$ (for small and large z) from Eq. (83) is far from trivial. Fortunately, this can be done, as we demonstrate it below.

1. *The limit $z \to 0$*

The small z limit of $V_\mu(z)$ corresponds to the large w limit in Eq. (83). To extract the large w behavior of $J_\mu(w)$ in Eq. (83), we rewrite it as

$$\begin{aligned} J_\mu(w) &= \exp\left[-\frac{1}{\pi}\int_0^\infty \frac{du}{1+u^2}\,\ln\left((a_\mu\,w\,u)^\mu\,(1+(a_\mu\,w\,u)^{-\mu}\right)\right] \\ &= \exp\left[-\frac{\mu}{\pi}\int_0^\infty \frac{du}{1+u^2}\,\ln(a_\mu\,w\,u) - \frac{1}{\pi}\int_0^\infty \frac{du}{1+u^2}\,\ln\left(1+(a_\mu\,w\,u)^{-\mu}\right)\right] . \end{aligned} \tag{86}$$

The first integral on the rhs in Eq. (86) can be done exactly and gives simply $(\pi/2)\,\ln(a_\mu\,w)$. Hence, we get

$$J_\mu(w) = \frac{1}{(a_\mu\,w)^{\mu/2}}\,\exp\left[-I_\mu(a_\mu\,w)\right]; \quad \text{where} \quad I_\mu(w) = \frac{1}{\pi}\int_0^\infty \frac{du}{1+u^2}\,\ln\left(1+(w\,u)^{-\mu}\right) . \tag{87}$$

Note that, so far, we have not taken the $w \to \infty$ limit and Eq. (87) is exact for all w. The purpose of the above manipulation was just to extract the leading singularity $w^{-\mu/2}$ of $J_\mu(w)$. It now remains to determine the large w behavior of $I_\mu(w)$.

A careful analysis of the large w limit of the integral $I_\mu(w)$ in Eq. (87) gives the following asymptotic behaviors (see Appendix A for details)

$$I_\mu(w) = \begin{cases} \dfrac{1}{\sin(\pi/\mu)\,w} + O(w^{-2}) & \text{when } \ 1 < \mu \leq 2 , \\ \dfrac{1}{\pi\,w}\,\ln(w) + O(w^{-1}) & \text{when } \ \mu = 1 , \\ \dfrac{1}{2\,\cos(\pi\,\mu/2)\,w^\mu} + O\left(w^{-\min(1,2\,\mu)}\right) & \text{when } 0 < \mu < 1 . \end{cases} \tag{88}$$

Using these results in Eq. (87), we find that for all $0 < \mu \leq 2$,

$$J_\mu(w) \sim \frac{1}{(a_\mu\,w)^{\mu/2}} \qquad \text{for } w \to +\infty . \tag{89}$$

Hence, from Eq. (83) we get

$$\int_0^\infty dy\,e^{-y}\,y^{1/\mu}\int_0^\infty dz\,V_\mu(z)\,e^{-w\,y^{1/\mu}\,z} \sim \frac{1}{a_\mu^{\mu/2}\,w^{1+\mu/2}} \qquad \text{for } w \to +\infty . \tag{90}$$

In order for both sides of Eq. (90) to have the same scaling $w^{-1-\mu/2}$ as $w \to +\infty$, it turns out that $V_\mu(z) \sim \gamma_\mu\, z^{\mu/2}$ as $z \to 0$, to be verified a posteriori and the unknown prefactor γ_μ to be determined. Indeed, substituting this anticipated behavior on the lhs of Eq. (90) and performing the integrals we find

$$\gamma_\mu \int_0^\infty dy e^{-y}\, y^{1/\mu} \int_0^\infty dz\, z^{\mu/2}\, e^{-w\, y^{1/\mu}\, z} = \frac{\gamma_\mu\, \sqrt{\pi}\, \Gamma(1+\mu/2)}{w^{1+\mu/2}}\,, \tag{91}$$

justifying this small z behavior of $V_\mu(z)$. Cancelling $w^{-(1+\mu/2)}$ from both sides, we see that $\gamma_\mu = A_\mu$, where A_μ is given in Eq. (16). Hence, finally, for all $0 < \mu \leq 2$, the asymptotic behavior of $V_\mu(z)$ for small z is given by

$$V_\mu(z) \sim A_\mu\, z^{\mu/2} \text{ for } z \to 0, \quad \text{where} \quad A_\mu = \frac{a_\mu^{-\mu/2}}{\sqrt{\pi}\, \Gamma(1+\mu/2)}\,, \tag{92}$$

as announced in Eq. (23).

2. *The limit $z \to \infty$*

The large z limit of $V_\mu(z)$ corresponds to the small w limit in Eq. (83). Clearly, from the expression of $J_\mu(w)$ in Eq. (83) one has $J_\mu(0) = 1$ and the large z behavior of $V_\mu(z)$ is actually determined by the leading singular correction in $J_\mu(w)$ as $w \to 0$. This correction depends on whether $0 < \mu < 1$, $1 < \mu < 2$, or $\mu = 1$. One finds (see [26] for details)

$$J_\mu(w) \sim \begin{cases} 1 - b_\mu\, w^\mu\,, \ 0 < \mu < 1\,, \\ \\ 1 + \dfrac{a_1}{\pi}\, w\, \ln w\,, \ \mu = 1\,, \qquad\qquad \text{for } w \to 0 \\ \\ 1 - \alpha_\mu\, w - b_\mu\, w^\mu\,, \ 1 < \mu \leq 2\,, \end{cases} \tag{93}$$

where the amplitudes α_μ and b_μ are given by [26]

$$\alpha_\mu = J'_\mu(0) = -\frac{a_\mu}{\sin(\pi/\mu)} \quad , \quad b_\mu = \frac{a_\mu^\mu}{2\cos(\mu\pi/2)}\,. \tag{94}$$

To get the large z behavior of $V_\mu(z)$ from Eqs. (83) and (93) it is convenient to introduce its Laplace transform

$$\tilde{V}_\mu(\rho) = \int_0^\infty V_\mu(z) e^{-\rho\, z}\, dz\,, \tag{95}$$

so that the equation determining $V_\mu(z)$ in Eq. (83) reads

$$\int_0^\infty dy\, e^{-y} y^{1/\mu}\, \tilde{V}_\mu(w\, y^{1/\mu}) = \frac{1}{w} J_\mu(w)\,. \tag{96}$$

From this equation, and the small w behavior of $J_\mu(w)$ in the first line of Eq. (93) one can determine the small ρ behavior of $\tilde{V}_\mu(\rho)$. Again, the three cases $0 < \mu < 1$, $1 < \mu < 2$ and $\mu = 1$ have to be analyzed separately.

$0 < \mu < 1$. In this case, by inserting a power law behavior of $\tilde{V}_\mu(w\, y^{1/\mu})$, valid for small w, on the lhs of Eq. (96) and using the small w expansion of $J_\mu(w)$ (93) on the rhs of Eq. (96), one obtains by matching the powers of w on both sides:

$$\tilde{V}_\mu(\rho) \sim \frac{1}{\rho} - b_\mu\, \rho^{\mu-1} \qquad \text{for } \rho \to 0\,, \tag{97}$$

where b_μ is given in Eq. (94). Using then a Tauberian theorem, one finds

$$V_\mu(z) \sim 1 - \tilde{A}_\mu\, z^{-\mu} \text{ for } z \to +\infty \quad , \quad \text{where} \quad \tilde{A}_\mu = \frac{b_\mu}{\Gamma(1-\mu)} = \frac{a_\mu^\mu}{2\,\Gamma(1-\mu)\,\cos\mu\pi/2}\,. \tag{98}$$

Finally, using Euler's reflection formula $\Gamma(1-\mu)\Gamma(\mu) = \pi/\sin(\pi\mu)$ (valid for $\mu \notin \mathbb{Z}$) one obtains the result announced in Eq. (23).

$1 < \mu < 2$. The same analysis can be done in this case, where the small w behavior of $J_\mu(w)$ is now given by the third line of Eq. (93). We get

$$\tilde{V}_\mu(\rho) \sim \frac{1}{\rho} - \frac{\alpha_\mu}{\Gamma(1+1/\mu)} - b_\mu\, \rho^{\mu-1} \qquad \text{for } \rho \to 0\ , \tag{99}$$

where α_μ and b_μ are given in Eq. (94). The leading term in this expansion, i.e., $1/\rho$, is the same as the one obtained for $0 < \mu < 1$ in Eq. (97). The first (regular) correction is a constant term associated with the regular part of the scaling function that decays rapidly for large z (note that there was a typo in Eq. (B24) of Ref. [26]). Its contribution to the large z behavior is negligible compared to the one of the third term in Eq. (99) which is the first singular correction giving rise to the algebraic decay

$$V_\mu(z) \sim 1 - \tilde{A}_\mu\, z^{-\mu} \qquad \text{for } z \to +\infty\ , \tag{100}$$

as announced in Eq. (23).

$\mu = 1$. This case needs to be analyzed separately because of the presence of logarithmic corrections in the small w behavior of $J_1(w)$ (see the second line of Eq. (93)). By using this asymptotic behavior in Eq. (96) we find that $\tilde{V}_1(\rho)$ behaves, for small ρ, as

$$\tilde{V}_1(\rho) \sim \frac{1}{\rho} + \frac{a_1}{\pi} \ln \rho \qquad \text{for } \rho \to 0\ , \tag{101}$$

from which one straightforwardly obtains the large z behavior

$$V_1(z) \sim 1 - \tilde{A}_1\, z^{-1} \text{ for } z \to +\infty \quad , \quad \text{where} \quad \tilde{A}_1 = \frac{a_1}{\pi}\ , \tag{102}$$

as announced in Eq. (23).

To conclude, we point out that, while the small w behavior of $J_\mu(w)$ differs in the three cases $0 < \mu < 1$, $1 < \mu < 2$ or $\mu = 1$, the functional dependence of the amplitude $\tilde{A}_\mu$ in Eq. (23) on the parameter μ is the same on the whole interval $\mu \in (0, 2)$ (this fact was actually overlooked in Ref. [26]).

VI. CONCLUSION

In this paper we have investigated the persistence, or survival probability, for long random walks and Lévy flights as a function of the starting position. Assuming that the walker starts at some $x_0 \geq 0$, we have identified two different regimes depending on how x_0 scales with the number of steps n in the walk. These two regimes determine the late time behavior of the survival probability as given by Eq. (10).

The classical, or standard, scaling regime is defined by $x_0 = O(n^{1/\mu})$ for large n. It is well-known that with the resolution of the standard rescaled variables, the discrete-time random walk appears as a continuous time random process for which the persistence goes to zero with the starting point [see Eq. (4)]. On the other hand, in the inner, or quantum, regime defined by $x_0 = O(1)$, the persistence goes to a finite (non-zero) value as x_0 goes to zero, as given by the Sparre Andersen results in Eqs. (8) and (9). Note that with the resolution of the standard rescaled variables, this latter regime lives inside a thin boundary layer of width $\sim n^{-1/\mu} \ll 1$ located near (and above) the origin, hence the name of 'inner' regime. (The fact that the discrete-time nature of the walk can no longer be neglected in this boundary layer justifies the alternative name of 'quantum' regime we have also used). It is the very existence of this boundary layer, in which the quantum regime takes the place of the classical one, that lifts the apparent paradox between the classical and Sparre Andersen results [Eqs. (4) and (9), respectively]. For any fixed, arbitrarily large, n there is always a starting position $x_0 > 0$ (or $x_0/n^{1/\mu} > 0$ in the rescaled variables) below which the second line in Eq. (10) must be replaced with the first line, leading to the Sparre Andersen limit (9) which always gives the (unique) correct result for $x_0 = 0$.

By a careful analysis of the asymptotics of the functions $U(x_0)$ and $V_\mu(z)$ appearing on the rhs of Eq. (10), we have proved that the classical and quantum regimes match smoothly near there common limit of validity, in the sense that the large x_0 limit of $U(x_0)$ in the first line of Eq. (10) (inner regime) coincides with the small $x_0/n^{1/\mu}$ limit of $V_\mu(x_0/n^{1/\mu})$ in the second line of Eq. (10) (standard scaling regime). Our analysis also shows that there are only two scales in the large n behavior of $q(x_0, n)$, namely $x_0 = O(1)$ and $x_0 = O(n^{1/\mu})$.

Indeed, this kind of quantum to classical crossover, as a function of temperature, also occurs in real quantum problems. For instance, for N non-interacting fermions in a one-dimensional harmonic trap of frequency ω, the statistics of the kinetic energy, as a function of temperature T, exhibits two scales [41]: one when it is of the order of the energy gap between single particle levels ($k_B\,T \sim \hbar\omega$), and the other one when it is of the order of the Fermi energy E_F ($k_B\,T \sim N\,\hbar\omega \sim E_F$). When $k_B\,T = O(\hbar\omega)$, quantum fluctuations dominate the statistics of the kinetic energy while for $k_B\,T = O(N\hbar\omega)$ the classical/thermal fluctuations take over. The crossover between the quantum and the classical regimes in this quantum problem is very much reminiscent, at least qualitatively, to the crossover described in this paper.

As mentioned at the end of the introduction, while the spirit of this paper is that of a review, there are nevertheless a few new results that we have not seen in the published literature. For the reader's sake, we provide here a list of these new results: (i) The existence of two scales of x_0 (the discrete 'quantum' regime where $x_0 \sim O(1)$ and the 'classical' scaling regime where $x_0 \sim O(n^{1/\mu})$) in the asymptotic behavior of $q(x_0, n)$ as a function of x_0, as well as the demonstration of the smooth matching between these two different scales, is new to the best of our knowledge. (ii) The results for $q(x_0, n)$ in Eqs. (10), with the expression for $U(x_0)$ in Eq. (11) appear to be new. Similarly, the asymptotic properties of $U(x_0)$ in Eq. (13), along with the general expressions for the constants in Eqs. (14), (15) and (16) are also new. (iii) The expression in Eq. (20) for the constant C_2, valid for arbitrary symmetric and continuous jump PDF $f(\eta)$ is new, and for the particular case of the Milne jump PDF in Eq. (60) our general result in Eq. (20) provides a new analytical expression for the Hopf constant $C_2^{\rm Hopf}$ in Eq. (65) that seems different from the other known expressions for this famous constant in the literature.

Appendix A: The large w behavior of $I_\mu(w)$

In this appendix, we analyse the large w behavior of the following integral

$$I_\mu(w) = \frac{1}{\pi}\int_0^\infty \frac{du}{1+u^2}\,\ln\left(1+(wu)^{-\mu}\right)\,; \qquad 0<\mu\le 2\,. \tag{A1}$$

The case $1<\mu\le 2$: We first partition the integral in Eq. (A1) into two separate integrals as follows

$$\begin{aligned} I_\mu(w) &= \frac{1}{\pi}\int_0^\infty du\,\ln\left(1+(wu)^{-\mu}\right)\left[1-\frac{u^2}{1+u^2}\right] \\ &= \frac{1}{\pi w}\int_0^\infty dq\,\ln(1+q^{-\mu}) - \frac{1}{\pi}\int_0^\infty \frac{du\,u^2}{1+u^2}\,\ln\left(1+(wu)^{-\mu}\right) = S_1(w)+S_2(w) \end{aligned} \tag{A2}$$

where in the first integral we have made a change of variable $wu = q$. Note that the first integral $S_1(w)$ is convergent for $1<\mu\le 2$, and yields the leading behavior as $w\to\infty$

$$S_1(w) = \frac{1}{\sin(\pi/\mu)\,w}\,. \tag{A3}$$

The second integral $S_2(w)$ provides only subleading corrections for large w. The first subleading term can be estimated by expanding the logarithm in the integrand in $S_2(w)$ and keeping the first term

$$S_2(w) \approx -\frac{w^{-\mu}}{\pi}\int_0^\infty du\frac{u^{2-\mu}}{1+u^2} = \frac{w^{-\mu}}{2\,\cos(\pi\mu/2)}\,. \tag{A4}$$

Evidently, the integral is convergent for $1<\mu\le 2$. Adding the two integrals then yields the leading large w behavior of $I_\mu(w)$ for $1<\mu\le 2$

$$I_\mu(w) = \frac{1}{\sin(\pi/\mu)\,w} + O(w^{-\mu})\,, \qquad 1<\mu\le 2\,. \tag{A5}$$

The case $\mu = 1$: In this case

$$I_1(w) = \frac{1}{\pi}\int_0^\infty \frac{du}{1+u^2}\,\ln\left(1+\frac{1}{wu}\right)\,. \tag{A6}$$

To extract the leading large w behavior, it is convenient to first take the derivative if $I_1(w)$ with respect to w. The resulting integral for $I_1'(w) = dI_1(w)/dw$ can be performed exactly. We get

$$I_1'(w) = -\frac{1}{\pi w}\int_0^\infty \frac{du}{(1+u^2)(1+wu)} = -\frac{\pi + 2w\ln(w)}{2\pi w(1+w^2)}\,. \tag{A7}$$

We now expand the rhs of Eq. (A7) for large w. This gives

$$I_1'(w) = \frac{-\ln w}{\pi w^2}\left[1 + \frac{\pi}{2w\ln w} + O(w^{-2})\right]\,. \tag{A8}$$

Integrating back, using $I_1(\infty) = 0$, immediately gives the large w asymptotics

$$I_1(w) = \frac{\ln w}{\pi w} + O(w^{-1})\,, \qquad \mu = 1\,. \tag{A9}$$

The case $0 < \mu < 1$: In this case, we again separate the integral $I_\mu(w)$ in Eq. (A1) into two parts, but in a different way from in Eq. (A2), as follows

$$\begin{aligned} I_\mu(w) &= \frac{1}{\pi}\int_0^\infty \frac{du}{1+u^2}\left[\ln\left(1+(wu)^{-\mu}\right) - (wu)^{-\mu} + (wu)^{-\mu}\right] \\ &= \frac{w^{-\mu}}{\pi}\int_0^\infty \frac{du\,u^{-\mu}}{1+u^2} + \frac{1}{\pi}\int_0^\infty \frac{du}{1+u^2}\left[\ln\left(1+(wu)^{-\mu}\right) - (wu)^{-\mu}\right] \\ &= T_1(w) + T_2(w)\,. \end{aligned} \tag{A10}$$

The first integral $T_1(w)$ is convergent for all $0 < \mu < 1$ and yields the leading behavior for large w

$$T_1(w) = \frac{w^{-\mu}}{\pi}\int_0^\infty \frac{du\,u^{-\mu}}{1+u^2} = \frac{1}{2\cos(\mu\pi/2)\,w^\mu}\,, \qquad 0 < \mu < 1\,. \tag{A11}$$

The second integral $T_2(w)$ yields subleading terms for large w. To extract the leading behavior of $T_2(w)$, we first make a change of variable $wu = q$ in the expression of $T_2(w)$ in Eq. (A10). This gives

$$T_2(w) = \frac{w}{\pi}\int_0^\infty \frac{dq}{q^2+w^2}\left[\ln(1+q^{-\mu}) - q^{-\mu}\right]\,. \tag{A12}$$

We note that the term $\ln(1+q^{-\mu}) - q^{-\mu} \sim q^{-2\mu}$ for large q. Thus, for large w, if we approximate $q^2 + w^2 \approx w^2$ in the denominator of the integrand in Eq. (A12), the resulting integral remains convergent, provided $1/2 < \mu < 1$. Thus in the range $1/2 < \mu < 1$, we get, for large w, the leading behavior of $T_2(w)$ as

$$T_2(w) \approx \frac{1}{\pi w}\int_0^\infty dq\,\left[\ln(1+q^{-\mu}) - q^{-\mu}\right] = O(1/w)\,; \qquad 1/2 < \mu < 1\,. \tag{A13}$$

If however $0 < \mu < 1/2$, the integral is not convergent and this approximation does not work. In this case, one can re-start from the expression of $T_2(w)$ in Eq. (A12) and re-write the integral as

$$\begin{aligned} T_2(w) &= \frac{w}{\pi}\int_0^\infty \frac{dq}{q^2+w^2}\left[\ln(1+q^{-\mu}) - q^{-\mu} + \frac{1}{2}q^{-2\mu} - \frac{1}{2}q^{-2\mu}\right] \\ &= -\frac{w}{2\pi}\int_0^\infty \frac{dq\,q^{-2\mu}}{q^2+w^2} + \frac{w}{\pi}\int_0^\infty \frac{dq}{q^2+w^2}\left[\ln(1+q^{-\mu}) - q^{-\mu} + \frac{1}{2}q^{-2\mu}\right] \\ &= T_{21}(w) + T_{22}(w)\,. \end{aligned} \tag{A14}$$

The first integral $T_{21}(w)$ is convergent for all $0 < \mu < 1/2$ and gives after a change of variable $q = wv$

$$T_{21}(w) = -\frac{w^{-2\mu}}{2\pi}\int_0^\infty \frac{dv\,v^{-2\mu}}{1+v^2} = -\frac{w^{-2\mu}}{4\cos(\mu\pi)}\,; \qquad 0 < \mu < 1/2\,. \tag{A15}$$

One can then analyse the second integral $T_{22}(w)$ in Eq. (A14) in a similar way as before, namely, we can approximate $q^2 + w^2 \approx w^2$ for large w in the denominator of $T_{22}(w)$. The resulting integral is convergent, provided $1/3 < \mu < 1/2$. This gives

$$T_{22}(w) \approx \frac{1}{\pi w}\int_0^\infty dq\left[\ln(1+q^{-\mu}) - q^{-\mu} - \frac{1}{2}q^{-2\mu}\right] = O(\frac{1}{w})\,; \qquad 1/3 < \mu < 1/2\,. \tag{A16}$$

For $\mu < 1/3$, one can again repeat the same procedure (of subtracting the singular terms in the expansion of $\ln(1+q^{-\mu})$ for large q) and it is easy to see that $T_{22}(w) \sim w^{-3\mu}$ for $1/4 < \mu < 1/3$ etc. Thus, adding $T_{21}(w)$ and $T_{22}(w)$, we find that the leading order behavior of $T_2(w)$ is given by

$$\begin{aligned} T_2(w) &\sim w^{-1}\,, \quad \text{for} \quad 1/2 < \mu < 1 \\ &\sim w^{-2\mu}\,, \quad \text{for} \quad 0 < \mu < 1/2\,. \end{aligned} \tag{A17}$$

The asymptotic large w behaviors in Eq. (A17) can be put together for all $0 < \mu < 1$ simply as

$$T_2(w) \sim w^{-\min(1,2\mu)}\,, \qquad 0 < \mu < 1\,. \tag{A18}$$

Finally, adding $T_1(w)$ in Eq. (A11) and $T_2(w)$ in Eq. (A18), we get the large w asymptotic behavior of $I_\mu(w)$ for $0 < \mu < 1$

$$I_\mu(w) = \frac{1}{2\cos(\mu\pi/2)\, w^\mu} + O\left(w^{-\min(1,2\mu)}\right)\,, \qquad 0 < \mu < 1\,. \tag{A19}$$

Summarizing, we find the following large w asymptotics of $I_\mu(w)$ in Eq. (A1) for all $0 < \mu \leq 2$

$$I_\mu(w) = \begin{cases} \dfrac{1}{\sin(\pi/\mu)\, w} + O(w^{-\mu}) & \text{when } \; 1 < \mu \leq 2 \\ \\ \dfrac{1}{\pi\, w}\, \ln(w) + O(w^{-1}) & \text{when } \mu = 1\,, \\ \\ \dfrac{1}{2\,\cos(\pi\,\mu/2)\, w^\mu} + O\left(w^{-\min(1,2\,\mu)}\right) & \text{when } 0 < \mu < 1\,, \end{cases} \tag{A20}$$

as given in Eq. (88) in the text.

Appendix B: Survival probability $q(x_0, n)$ for lattice random walk with ± 1 jumps

Here we consider a random walker on a 1-d lattice (with integer points), starting at the initial position x_0 (note that x_0 is a non-negative integer). At each discrete time step, the walker jumps by either $+1$ or -1, chosen with equal probability $1/2$. This corresponds to a jump PDF of the form, $f(\eta) = \frac{1}{2}\delta(\eta - 1) + \frac{1}{2}\delta(\eta + 1)$, which is symmetric but not *continuous*. Hence, the general results derived in this paper for symmetric and continuous jump density cannot be directly applied to this case. However, this case can be worked out separately as we show in this Appendix.

Let $q(x_0, n)$ denote the survival probability, i.e., the probability that the walker, starting at x_0 ($x_0 \geq 0$), stays non-negative up to step n. One can easily write down a recursion relation for $q(x_0, n)$

$$q(x_0, n) = \frac{1}{2}\left[q(x_0 - 1, n - 1) + q(x_0 + 1, n - 1)\right]\,, \quad x_0 \geq 0 \tag{B1}$$

with the boundary condition: $q(-1, n) = 0$. The initial condition is: $q(x_0, 0) = 1$ for all $x_0 \geq 0$. To solve this recursion, we define the generating function

$$\tilde{q}(x_0, s) = \sum_{n=0}^{\infty} q(x_0, n)\, s^n\,. \tag{B2}$$

Then, the generating function satisfies the inhomogeneous equation for all $x_0 \geq 0$

$$\tilde{q}(x_0, s) = 1 + \frac{s}{2}\left[\tilde{q}(x_0 + 1, s) + \tilde{q}(x_0 - 1, s)\right] \tag{B3}$$

with the boundary conditions: $q(x_0 = -1, s) = 0$ and $q(x_0 \to \infty, s)$ non-divergent. By making a shift, $\tilde{q}(x_0, s) = (1-s)^{-1} + \tilde{r}(x_0, s)$ that gets rid of the inhomogeneous constant term in Eq. (B3) and solving the resulting homogeneous equation for $\tilde{r}(x_0, s)$, it is easy to see that the most general solution to Eq. (B3) is given by

$$\tilde{q}(x_0, s) = \frac{1}{1 - s} + A\,[\lambda_+(s)]^{x_0} + B\,[\lambda_-(s)]^{x_0} \tag{B4}$$

where $\lambda_\pm(s) = (1 \pm \sqrt{1-s^2})/s$ and A and B are two arbitrary constants. The boundary condition that $\tilde{q}(x_0 \to +\infty, s)$ is non-divergent forces the constant $A = 0$. The other boundary condition $\tilde{q}(-1, s) = 0$ fixes the constant $B = -\lambda_-(s)/(1-s)$. Hence, the full exact solution is then given by

$$\tilde{q}(x_0, s) = \frac{1 - (\lambda_-(s))^{x_0+1}}{1-s} = \frac{1}{1-s}\left[1 - \left(\frac{1-\sqrt{1-s^2}}{s}\right)^{x_0+1}\right], \quad \text{for all} \quad x_0 \geq 0\,. \tag{B5}$$

It is now easy to extract the asymptotic behavior of $q(x_0, n)$ for large n by analyzing Eq. (B5) near $s = 1$. We consider again the two regimes (i) discrete 'quantum' regime where $x_0 \sim O(1)$ is fixed, and $n \to \infty$ and (ii) 'classical' scaling regime where $x_0 \sim \sqrt{n}$ as $n \to \infty$, separately.

Regime I: $x_0 \sim O(1)$. Setting $s = 1 - p$ and expanding the right hand side of Eq. (B5) in powers of p (while keeping x_0 fixed) gives

$$\tilde{q}(x_0, s = 1-p) = \frac{\sqrt{2}(x_0+1)}{\sqrt{p}} - (x_0+1)^2 + O(\sqrt{p})\,. \tag{B6}$$

Hence, inverting the generating function, one gets the leading asymptotic behavior of $q(x_0, n)$ for large n with fixed x_0 as

$$q(x_0, n) = \frac{1}{\sqrt{n}}\, U_{\rm lw}(x_0)\,, \quad \text{where} \quad U_{\rm lw}(x_0) = \sqrt{\frac{2}{\pi}}\,(x_0+1)\,, \tag{B7}$$

where the subscript 'lw' stands for the lattice walk. Thus, in the 'quantum' regime, $q(x_0, n)$ behaves in the same way as in Eq. (10) of the main paper valid for continuous and symmetric jump distribution, except that the scaling function $U(x_0)$ is different and exactly given by Eq. (B7) for all $x_0 \geq 0$.

Regime II: $x_0 \sim \sqrt{n}$ with $z = x_0/\sqrt{n}$ fixed. In this case, seeting $s = 1-p$ with $p \to 0$, and $x_0 \to \infty$ but keeping the product $x_0\sqrt{p}$ fixed, the right hand side of Eq. (B5), to leading order, is given by

$$\tilde{q}(x_0, s = 1-p) \approx \frac{1 - e^{-\sqrt{2p}(x_0+1)}}{p}\,. \tag{B8}$$

Inverting the laplace transform with respect to p, one gets, to leading order in the scaling regime

$$q(x_0, n) \to V_{\rm lw}\left(\frac{x_0}{\sqrt{n}}\right), \quad \text{where} \quad V_{\rm lw}(z) = \mathrm{erf}\left(\frac{z}{\sqrt{2}}\right). \tag{B9}$$

To summarize, in the case of a ± 1 lattice walk, one gets the following large n behaviors for the survival probability

$$q(x_0, n) \sim \begin{cases} \dfrac{1}{\sqrt{n}}\, U_{\rm lw}(x_0) \quad \text{for} \quad n \to +\infty \quad \text{and} \quad x_0 = O(1)\,, \\ \\ V_{\rm lw}\left(\dfrac{x_0}{n^{1/2}}\right) \quad \text{for} \quad n \to +\infty \quad \text{and} \quad x_0 = O(n^{1/2})\,, \end{cases} \tag{B10}$$

where

$$U_{\rm lw}(x_0) = \sqrt{\frac{2}{\pi}}\,(x_0+1) \quad \text{for all} \quad x_0 \geq 0\,, \tag{B11}$$

$$V_{\rm lw}(z) = \mathrm{erf}\left(\frac{z}{\sqrt{2}}\right). \tag{B12}$$

It is easy to check that the behaviors of $q(x_0, n)$ match smoothly at the boundary between the two regimes I and II. Taking $x_0 \gg 1$ in the discrete quantum regime, one gets $q(x_0, n) \approx \sqrt{2/\pi}\, x_0$. On the other hand, letting $x_0 \ll \sqrt{n}$ in the classical scaling regime and using $\mathrm{erf}(z) \to \frac{2}{\sqrt{\pi}}\, z$ as $z \to 0$, one gets the same expression $q(x_0, n) \approx \sqrt{2/\pi}\, x_0$,

ensuring a smooth matching between the two regimes. In Fig. 3, we show a plot of $q(x_0, n)$ for a lattice random walk of $n = 1000$ steps and compare it with our analytical predictions in Eqs. (B11) and (B12).

[1] W. Feller, *An Introduction to Probability Theory and its Applications*, Vol. 1 and 2 (New York, Wiley, 1968).
[2] S. Redner, *A guide to first-passage processes* (Cambridge University Press, Cambridge, 2001).
[3] S. N. Majumdar, Curr. Sci. **77**, 370 (1999).
[4] A. J. Bray, S. N. Majumdar and G. Schehr, Adv. Phys. **62**, 225 (2013).
[5] F. Aurzada and T. Simon, Lévy matters V:183-221, *Lecture Notes in Math* 2149, Springer, (2015).
[6] J.-P. Bouchaud and A. Georges, Phys. Rep. **195**, 127 (1990).
[7] R. Metzler and J. Klafter, Phys. Rep. **339**, 1 (2000).
[8] E. Sparre Andersen, Mathematica Scandinavica **2**, 195 (1954).
[9] E. A. Milne, Monthly Notices Royal Astron. Soc. **81**, 361 (1921).
[10] G. Placzek and W. Seidel, Phys. Rev. **72**, 550 (1947).
[11] S. Finch, *Radiative Transfer Equation*, `goo.gl/Zn0lpd`.
[12] G. Zumofen and J. Klafter, Phys. Rev. E **51**, 2805 (1995).
[13] A. Comtet and S. N. Majumdar, J. Stat. Mech.: Theory and Exp., P06013 (2005).
[14] S. N. Majumdar, Physica A, **389**, 4299 (2010).
[15] S. N. Majumdar, A. Comtet and R. M. Ziff, J. Stat. Phys. **122**, 833 (2006).
[16] R. M. Ziff, S. N. Majumdar, A. Comtet, J. Phys. C: Cond. Matter **19**, 065102 (2007).
[17] R. M. Ziff, J. Stat. Phys. **65**, 1217 (1991).
[18] G. Schehr and S. N. Majumdar, Phys. Rev. Lett. **108**, 040601 (2012).
[19] G. Schehr and S. N. Majumdar, *Exact record and order statistics of random walks via first-passage ideas*, in "First-Passage Phenomena and Their Applications", Eds. R. Metzler, G. Oshanin, S. Redner, World Scientific (2014), arXiv:1305.0639.
[20] S. N. Majumdar, Ph. Mounaix, and G. Schehr, Phys. Rev. Lett. **111**, 070601 (2013).
[21] S. N. Majumdar, Ph. Mounaix, and G. Schehr, J. Stat. Mech. P09013 (2014).
[22] Ph. Mounaix, G. Schehr, and S. N. Majumdar, J. Stat. Mech. P013303 (2016).
[23] Ph. Mounaix and G. Schehr, J. Phys. A: Math. Theor. **50**, 185001 (2017).
[24] N. H. Bingham, (2001), Random walk and fluctuation theory, Handbook of statistics **19**, 171 (2001).
[25] S. N. Majumdar and R. M. Ziff, Phys. Rev. Lett. **101**, 050601 (2008).
[26] G. Wergen, S. N. Majumdar, and G. Schehr, Phys. Rev. E, **86**, 011119 (2012).
[27] S. N. Majumdar, G. Schehr, and G. Wergen, J. Phys. A: Math. Theor. **45**, 355002 (2012).
[28] C. Godrèche, S. N. Majumdar and G. Schehr, J. Phys. A: Math. Theor. **47**, 255001 (2014).
[29] C. Godrèche, S. N. Majumdar and G. Schehr, J. Stat. Mech. P07027 (2015).
[30] C. Godrèche, S. N. Majumdar and G. Schehr, Phys. Rev. Lett., **117**, 010601 (2016).
[31] C. Godrèche, S. N. Majumdar and G. Schehr, J. Phys. A: Math. Theor. **50**, 333001 (2017).
[32] E. G. Coffman, Ph. Flajolet, L. Flato and M. Hofri, Probab. Eng. Inform. Sc. **12**, 373 (1998).
[33] We are grateful to V. V. Ivanov for sharing with us his private notes on the Hopf constant and the interesting history behind this constant.
[34] A. Kuznetsov, Stoch. Proc. Appl. **123**, 986 (2013).
[35] D. A. Darling, Trans. Amer. Math. Soc. **83**, 164 (1956).
[36] V. V. Ivanov, Astron. Astrophys. **286**, 328 (1994).
[37] F. Pollaczek, Comptes Rendus **234**, 2334 (1952).
[38] F. Spitzer, Trans. Am. Math. Soc. **82**, 323 (1956); Duke Math. J. **24**, 327 (1957).
[39] D. W. N. Stubbs and R. E. Weir, Mon. Not. R. Astron. Soc. **119**, 512 (1959).
[40] V. V. Ivanov, Nat. Bur. Standards, Spec. Publ. **385**, 125 (1973).
[41] J. Grela, S. N. Majumdar and G. Schehr, Phys. Rev. Lett. **119**, 130601 (2017).